Survey of shock-wave structures of smooth-particle granular flows

D. A. Padgett, A. P. Mazzoleni, and S. D. Faw

Phys. Rev. E **92**, 062209 — Published 28 December 2015

DOI: 10.1103/PhysRevE.92.062209

A Survey of Shock Wave Structures of Smooth Particle Granular Flows

D.A. Padgett,* A.P. Mazzoleni,† and S.D. Faw‡

Engineering Mechanics and Space Systems Laboratory,

Department of Mechanical and Aerospace Engineering,

North Carolina State University, Box 7910, Raleigh NC, 27695

Abstract

We show the effects of simulated supersonic granular flow made up of smooth particles passing over two prototypical bodies: a wedge and a disk. We describe a way of computationally identifying shock wave locations in granular flows and tabulate the shock wave locations for flow over wedges and disks. We quantify the shock structure in terms of oblique shock angle for wedge impediments and shock standoff distance for disk impediments. We vary granular flow parameters including upstream volume fraction, average upstream velocity, granular temperature, and the collision coefficient of restitution. Both wedges and disks have been used in the aerospace community as prototypical impediments to flowing air in order to investigate the fundamentally different shock structures emanating from sharp and blunt bodies, and we present these results in order to increase the understanding of the fundamental behavior of supersonic granular flow.

PACS numbers: 45.70.-n, 45.70.Qj, 47.40.Nm

* dapadget@ncsu.edu

† apmazzol@ncsu.edu

‡ sdfaw@ncsu.edu

I. INTRODUCTION

The phenomenon of shock waves in granular media [1–8] is well known and has been under study for some time. Granular media in certain density ranges behave as gases [9], and as such allow the propagation of shock waves from disturbances traveling at speeds greater than the characteristic sonic velocity of the granular gas. Shock waves and their structure are of great interest to the aerospace engineering community as the location of shock waves on aerodynamic bodies can have a large effect on the figures of merit for aerospace vehicle design [10]. Historically, the study of shock waves has provided an experimental tool for testing theoretical descriptions of the structure and movement of air and other fluids. We undertook the following research in order to more fully understand the effect of various granular flow parameters on shock structures in a granular flow and to organize this data in a way useful to us and to other researchers interested in investigating supersonic granular flow models.

The granular materials literature [11, 12] describes a class of granular shock waves in which the force of gravity plays a large role in the development and characteristics of the shock wave and Hákonardóttir, *et. al.* [13] theoretically describe "Mach-Beta-Theta" relations for oblique shock waves in granular materials in which the Froude number serves as an analog to the Mach number in typical gas oblique shock wave calculations. The influence of gravity is important in many applications of granular materials and therefore must be taken into account where appropriate; these shock waves are characterized by a hydraulic jump, or a change in the height of the granular material.

In contrast to hydraulic jump shock waves, Rericha [1] describes the Hele-Shaw arrangement for observing shock waves in granular flows. The Hele-Shaw arrangement results in a two-dimensional flow in which the average flow direction (upstream of the development of the shock wave) is parallel to the direction of gravity and the shock wave that is observed consists not of a hydraulic jump, but a rapid change in flow conditions in the spatial domain. In the Hele-Shaw arrangement, the gravitational force is not key to the development of the shock wave but does affect its shape. In granular Hele-Shaw flow, the force of gravity serves to accelerate the flow and can be computationally removed in simulations and shock waves will still develop. In this paper, we will focus on the two-dimensional Hele-Shaw geometry, and thus the shock waves described will consist of spatial changes in flow conditions and

not jumps in the height of the granular material. We are interested in the Hele-Shaw arrangement because there does not currently exist analogs to typical fluid Mach-Beta-Theta relations for the resulting shock waves and because this type of flow closely approximates two-dimensional fluid flow.

The two-dimensional granular flow geometry of interest in this paper has been studied both computationally and experimentally using a vertical Hele-Shaw cell [1] and using chutes to accelerate granular material over a horizontal surface [14]. The literature also describes both numerical and experimental studies into the flow of granular systems over various obstacles [15–17]; the numerical components of these simulations tend to use models which attempt to describe the experimental observations as completely as possible. In contrast, the goal of this paper is to investigate the response of granular gas systems to obstacles, and to investigate the resulting shock waves under a certain set of assumptions about granular systems. The work presented is in the same vein as that presented by Buchholtz and Pöschel [18] in their paper detailing both the computational issues inherent in, and the results of, modeling the interaction of granular streams with obstacles.

II. GRANULAR MODEL

In order to investigate the granular parameters which affect granular shock wave location, an idealized model of granular systems was chosen and computationally simulated. The granular system under study is a two dimensional system consisting of monodisperse spherical (2-D disk) particles of a given radius. Particles were allowed to collide with each other and with structures placed in the simulation space; in general, these structures were modeled using impermeable line segments, hereafter called "barriers" and served to impede granular motion. Collision both between particles and between a particle and a barrier were modeled using well known techniques used extensively in granular studies [19]. Because all collisions are assumed to take place between smooth bodies and there is no transfer of tangential motion or rotational motion between bodies, the angular momentum of each individual particle is conserved in the collision process; the simulation described is therefore a true two dimensional simulation which does not include a rotational degree of freedom.

A. Granular State Evolution

The granular simulation used to produce the results discussed in this paper is a deterministic, event-driven simulation which tracks the state of each particle in the system. The simulation is propagated by traversing an event tree which associates information concerning potential collisions (both particle-particle collisions and particle-barrier collisions) with the simulation time parameter at which the collision occurs. The event tree is initially populated at the beginning of the simulation. The simulation is provided with an initial particle state which is generated using an outside program; in most cases, the initial simulation state is specified using a custom MATLAB script. The simulation reads the initial state of the granular system and calculates an initial event tree by examining each particle in the simulation individually, calculating the time of the collision of the particle of interest with other particles in a user-defined area around the particle of interest, and placing each of these collisions in the event tree. Because the event tree associates collision information with collision time, the earliest occurring collision is easily determined.

Assuming that the earliest occurring collision happens at a time t_c after the current simulation time t_o, the states of the particles involved in the collision are modified to reflect the motion of the particles over the period from t_o to t_c as well as the instantaneous change in the velocity of the particles due to the collision. The states of the other particles in the system are changed to reflect the time change from t_o to t_c. Consistent with the most important assumption of granular systems, the granular particles interact with each other only through contact and not at a distance through gravitational or electrical forces. Therefore, the trajectory of a particle between collisions is dependent only on the external force acting on the system. Typically the external force is either zero or a constant (such as gravity), and the particle updating scheme involves the solution of an algebraic equation; determining the future state of a system of particles for which the algebraic form of the trajectory is known eliminates the need to computationally solve the differential equations of motion. For the simulations presented in this paper, the external forces are set to zero.

B. Simulation Algorithm

The code used to simulate the granular system described in this paper is an event-driven algorithm in which events (i.e., the collision of a particle with another particle or a boundary) are detected and ordered by the time until occurrence. The simulation can be broken down into four main steps: initialization, state modification, collision response, and collision detection. The first step, initialization, involves setting up the initial state of the particles in the simulation. For this research, a custom external script written in MATLAB was used to place particles in the simulation space such that the particles do not initially overlap. The number of particles placed in the simulation space is dependent on the user-specified volume fraction of the simulation. The initial velocities of the particles are sampled from a normal distribution of velocities resulting in a user-specified granular temperature (which is related to variance of the granular velocities). The particle velocities in the flow direction are also adjusted such that the average flow velocity is a user-defined multiple of the speed of sound (Mach number).

The barriers present in the simulation space are also defined during the initialization process. The simulation space is bounded by barriers in a square configuration. The sides of the square are impenetrable to the particles while the top and bottom boundaries are periodic; particles pass through the outflow boundary and are moved to the inflow boundary creating the circular effect needed to run the simulation for an indeterminate amount of time. The velocities of particles moved from the top boundary to the bottom boundary are resampled in order to ensure that the upstream flow conditions are consistent throughout the simulation; any "memory" of the flow condition after impinging on other particles or barriers are erased when a particle is moved back to the inflow boundary.

The final step in the initialization process is the initial population of the event list. The event queue is modeled as a C++ Standard Template Library Map structure, which acts as an associative array and orders elements in a tree-like structure. The event queue is ordered by the time at which the detected collisions occur, thus the soonest occurring collision is easily found. The event queue is initially populated by examining each particle in the simulation and calculating the times at which the distance between the particle of interest and other particles in the simulation is equal to the sum of the particle radii; the process is similar for the detection of particle-barrier collisions. In order to decrease the computational

expense associated with determining collision times, only the particles within a user-specified neighborhood of the particle of interest are tested for possible collisions; when examining whether a particle is going to collide with other particles, the most likely candidates for collision are the particles close to the particle of interest. The user-specified neighborhood size will henceforth be known as the collision search radius.

After the simulation is initialized and the initial event queue is populated, the simulation identifies the soonest-occurring collision. The states of the particles in the simulation are changed to reflect the passage of time $t_c - t_o$ and a collision handling algorithm is applied to the particles (or particle) participating in the collision. The collision handling algorithm [19] takes into account the coefficient of restitution of the collision, the properties of the particles, and the relative particle velocities to calculate the total impulse applied to each particle. The collisions are modeled as instantaneous changes in velocity, therefore, after the velocity impulse is calculated, the change is immediately applied to each particle velocity in each direction.

Because the velocities of the particle or particles involved in a collision change in both magnitude and direction, the collisions associated with those particles are no longer valid after the collision. Therefore, for each particle involved in a collision, it is necessary to both remove the associated collisions from the event queue and to repopulate the queue with new collisions that result from the new trajectory of the particle. The collision detection routine is therefore applied to the particles involved in the collision and the detected collisions are placed in the event queue. At this point, the simulation process is repeated by applying the collision handling algorithm to the soonest-occurring collision. The simulation continues until the simulation time reaches a user-defined maximum.

III. SHOCK WAVE DETECTION

Integral to the research discussed herein is the computational identification of the shock front position in the simulation space. Measuring the shock wave location is accomplished by monitoring the flow properties at points within the simulation and identifying changes in flow properties that correspond to shock waves. In order to monitor the flow properties as the simulation propagates, a measurement step is inserted into the algorithm and the measurements must be performed periodically. In practice, the measurement step is performed

at specific time intervals and the quantities measured include the particle volume fraction, the local average velocity in each direction, the local granular temperature, and the local Mach number. These quantities are calculated and stored as the simulation runs, and at the end of the simulation they are output for further post-processing.

Each of the quantities of interest are granular analogs to continuum properties. Because granular materials consist of a collection of particles, a process which maps the state of the granular system to continuum properties must be defined. In the simulation used in this research, this process involves spatial averaging of the granular state properties in order to estimate the volume fraction, average velocity, granular temperature, and local Mach number. The spatial averaging process makes use of a regular grid of points in the simulation space around which continuum variables are measured and at which continuum data are specified. The measurement step consists of identifying the particles located within a user-defined area around each of the grid points and using the state of each of the identified particles to determine the value of the desired quantity. In order to increase computational efficiency, the area around each point in which particles used in the continuum calculations are located is a square subspace of a user-defined side length centered at the point of interest.

The volume fraction measured is the two dimensional volume fraction, and is simply

$$\nu = \frac{\sum\limits_{i} \pi r_i^2}{A} \tag{1}$$

where r_i is the radius of a given particle and A is the area of the subspace in which the particles are located. The local average velocities are given by calculating the average of the velocities of the particles in the subspace of interest in each coordinate direction. The local granular temperature, T, is calculated by measuring the variance in the velocities of the particles within the subspace of interest using the equation in Ref. [20].

$$T = \frac{1}{D}\left(< v^2 > - < v >^2\right) = \frac{1}{D}\left(< \vec{v} \cdot \vec{v} > - < \vec{v} > \cdot < \vec{v} >\right) \tag{2}$$

where D is the dimension of the simulation space (2 in our case), v is the speed of each particle in the subspace of interest, $\vec{v}$ is the velocity of the particle, and quantities enclosed by an angle bracket are averaged over particles in the subspace. From Ref. [21], the granular

temperature is used to calculate the granular speed of sound c.

$$c = \sqrt{T\chi\left(1 + \frac{2}{3}\chi + \frac{\nu}{\chi}\frac{\partial\chi}{\partial\nu}\right)} \tag{3}$$

where χ, which is a correction factor to the equation of state, is given by

$$\chi = 1 + 2(1+e)G(\nu) \tag{4}$$

and G, the radial distribution function, is given by

$$G(\nu) = \left[1 - \left(\frac{\nu}{\nu_m}\right)^{4\nu_m/3}\right]^{-1} \tag{5}$$

as suggested by Goldshtein, *et al.* [2]. The random close packing volume fraction for disks [22], ν_m, is set to be 0.82 for the simulations performed. Mach number is defined as the ratio of the local average speed to the local speed of sound, i.e. Mach Number (Mach) $= |v|/c$ where c is the local speed of sound as defined in Eq. 3.

In order to use the above equations to estimate the desired quantities computationally, the particles in the user-defined area around a given point are identified using a nearest-neighbor test. The volume fraction and average velocities are the most direct computations. The results of these computations are used in the calculation of granular temperature, local sound speed, and local Mach number, all of which are stored in separate layers of a data array of dimension $N \times N \times M$ where N is the number of measurement grid points on each axis of the simulation space and M is the number of separate quantities to be measured at each point.

Local continuum quantities measured at one particular time using the techniques described make up a noisy data set. Spatial trends in the quantities of interest can be better determined by averaging the quantities measured at a particular point over time. In order to accomplish the desired time averaging, the $N \times N \times M$ data array is updated at regular intervals by adding quantities measured at the current time to the sum of the quantities measured at all previous times. The time averaging process decreases the contribution of transient noise in the continuum data, and thus is appropriate for evaluating steady-state spatial structures in the granular flow data such as shock waves emanating from an obstacle located in a granular flow. Figure 1 shows a dramatic change in the time-averaged volume fraction through the simulation space for supersonic granular flow over a wedge. We note

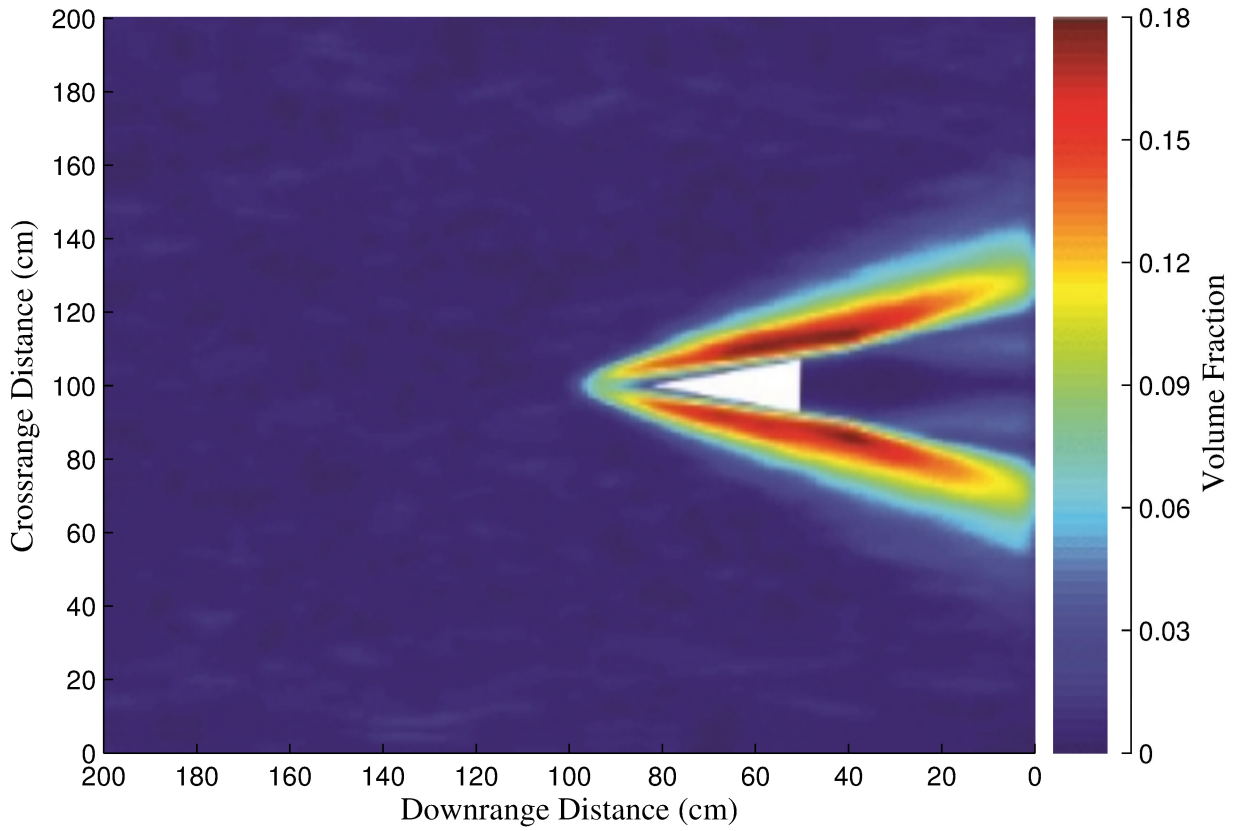

FIG. 1. (Color Online) Granular Simulation Results: Time-averaged volume fraction for granular flow over a wedge. The color (shading) indicates the local average volume fraction as calculated at each grid point. The granular flow impinges on a wedge with a 10^o half-angle. The largest volume fraction is concentrated around the upper and lower surface of the wedge.

that variation in color (non-uniformity in shading upstream) prior to impact suggests that energy in the flow is decreasing; however, we feel it to be small compared to the energy decrease at the shock. If this were not the case, we feel that there would be a noticeable volume fraction gradient between the "inlet" and the area that is affected by the shock wave.

Because of the relatively large size of the constituents of a granular flow, oblique granular shock waves tend to have a discernible structure on a larger scale than fluid shock waves, most of which are considered to form over a vanishingly small distance scale. The thickness of a granular shock structure necessitates a method of determining the location of the shock wave. In order to approximate the locations of the shock waves presented in this paper, the data is first smoothed using a low pass filter. The data along lines perpendicular to the obstruction causing the shock wave is then isolated from the two dimensional data. The

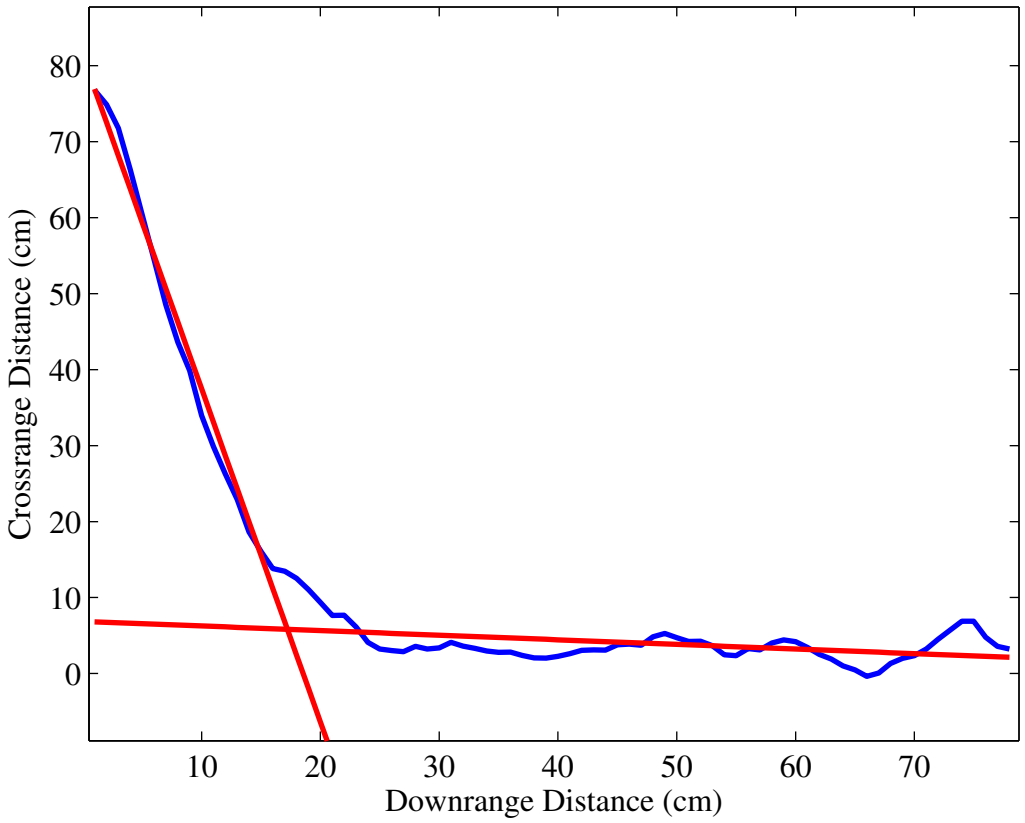

FIG. 2. (Color Online) An example of the shock-detection scheme along a given normal to the surface of the wedge shown in Fig.1. Both the data along the line and the two lines composing the minimum-error interpolation are shown. The intersection of the two interpolation lines is assumed to be the location of the shock wave.

process of determining the shock wave location along the normal line involves determining the point at which the data can be described as changing from relatively flat and constant to sloped. In order to find the transition point in the data, a two-part segmented linear regression is performed. The transition point between one linear segment and the other linear segment is taken to be the location of the shock wave. Both the data taken along the normal and the results of the segmented regression are shown in Fig. 2. The measured location of a shock wave over a wedge structure is shown in Fig. 3

IV. OBSERVED SHOCK PATTERNS

A. Flow Past a Wedge

Granular fluid flow impinging on a wedge shaped obstacle provides an interesting case study for the investigation of the supersonic properties of granular materials. Fluid flow past a wedge, especially in the supersonic regime, is a phenomenon that has been extensively studied in the world of aerodynamics. Under a broad range of flow conditions, the shock wave location resulting from supersonic flow over a wedge has a closed-form solution which has been confirmed experimentally [10]; such a result shows the power of the theoretical tools used to describe fluid flow. We explore supersonic granular flow over a wedge in order to compare and contrast standard fluid flow with supersonic granular fluid flow.

As discussed by Rericha [1, 20], the behavior of granular shock waves over a wedge has many similarities to shock waves arising from typical fluid flow. Both supersonic fluid and granular flow over a wedge result in the development of a shock wave emanating from the tip of the wedge and stretching at an angle through the flow; such shock waves are known as oblique shock waves in fluid mechanics. Figure 1 shows an example of the behavior of the steady-state time-averaged flow variables for a supersonic granular system flowing over a wedge. Oblique shock waves in fluid dynamics are characterized by the angle they form with respect to the average direction of fluid flow; therefore, we characterize granular oblique shock waves using the shock angle as the figure of merit. We calculate a linear regression of the predicted shock wave location shown in Fig. 3 and use the linear fit to generate an estimate of the oblique shock wave angle. We examine the response of the shock wave angle to the granular flow velocity, the granular temperature of the flow, the coefficient of restitution which characterizes collisions, and the volume fraction of the flow. When examining each of the listed variables, we hold the other variables constant at the default value given in Table I. The simulation space measures 1 meter on each side and the wedge length is held constant at 0.3 meters. Monodisperse particles of radii 0.001 meters constitute the simulated granular system.

Figure 4 shows the variation of the measured shock angle as the flow speed changes. Both the actual average flow speed (in meters per second) and the Mach number of the upstream flow are shown. The flow speed with the greatest variation in measured shock wave location

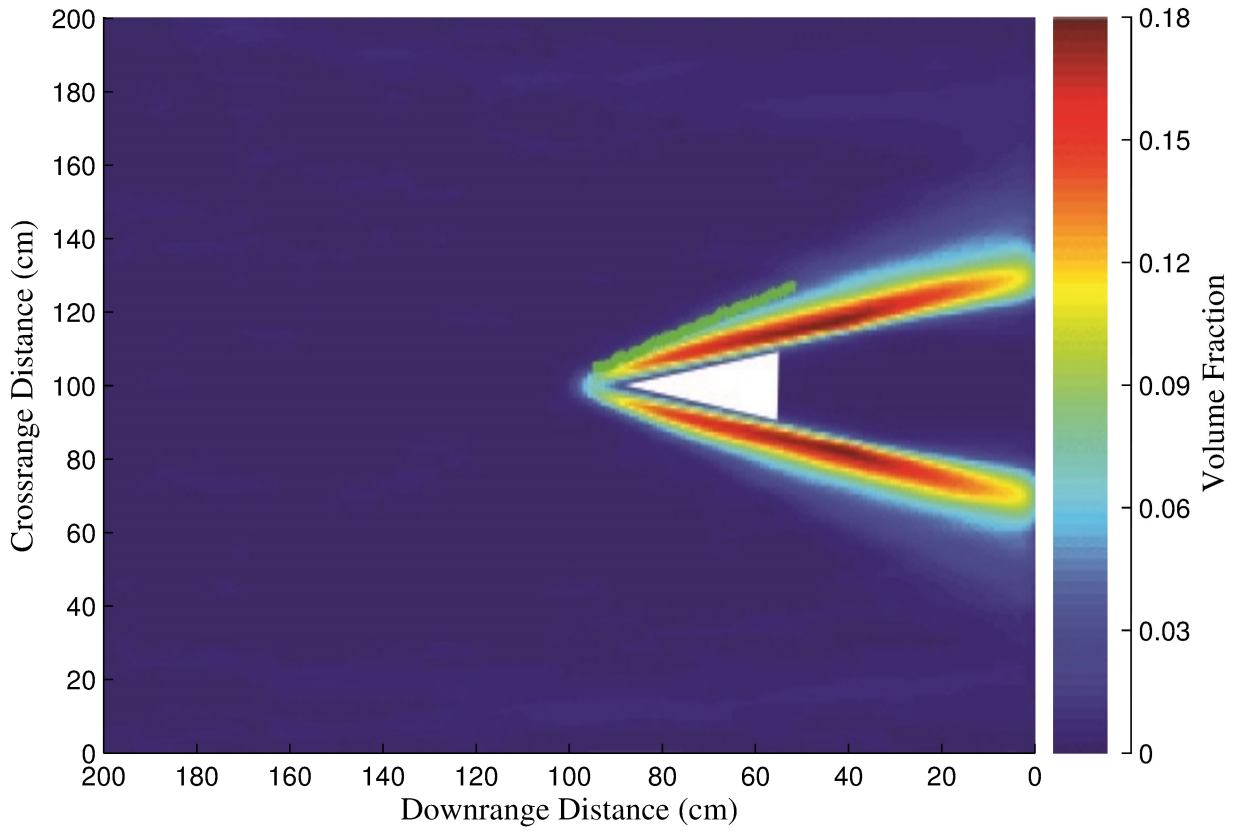

FIG. 3. (Color Online) Granular Simulation Results: The measured location of a shock wave over a wedge structure with a 10^o half-angle using two-part segmented linear regression. The color (shading) indicates the local average volume fraction as calculated at each grid point. The largest volume fraction is concentrated around the upper and lower surface of the wedge.

TABLE I.

Volume Fraction (ν)	0.03
Coefficient of Restitution (e)	0.9
Flow Velocity (v)	0.55 m/s
Granular Temperature (T)	0.01 m^2/s^2

corresponds to a flow Mach number of approximately 0.51. The shock detection algorithm described above is sensitive to changes in the spatial distribution of particles in the two dimensional simulation space; such a change in distribution occurs whenever the granular fluid flow speed is in the compressible range (considered to be at Mach numbers above 0.3 for typical fluids). We therefore interpret the erratic behavior and large margin of error

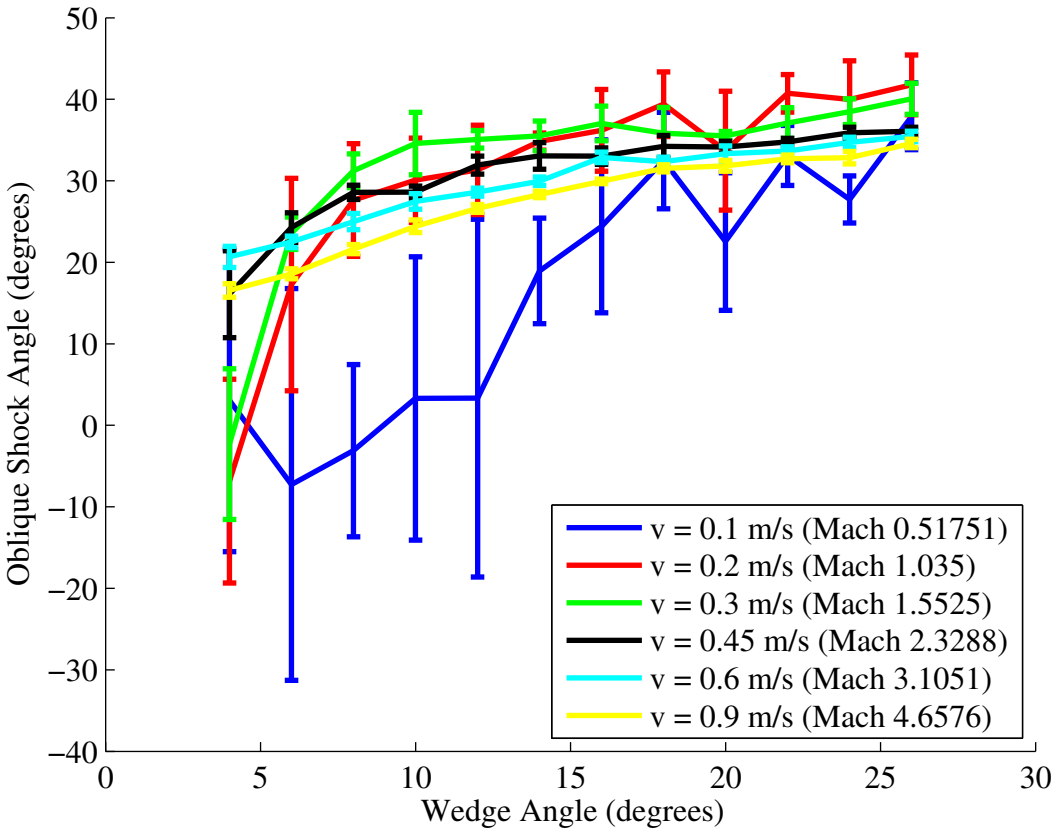

FIG. 4. (Color Online) The variation in oblique shock angle as a function of wedge angle and average flow velocity. Shock wave detection at Mach 0.51 is interpreted as an artifact of compressible flow, where shock waves are not fully formed, hence the large margin of error and erratic behavior. When viewing this figure in grayscale, note that at a wedge angle of 10^o, the curves proceed as follows from top to bottom: $v = 0.3, 0.2, 0.45, 0.6, 0.9, 0.1$ m/s, respectively.

associated with the shock detection at Mach 0.51 to the fact that the flow is compressible at this flow speed, but shock waves are not fully formed. At a Mach number of approximately 1, the measured oblique shock angle has a generally increasing trend with respect to wedge angle, but has a larger measured error at each wedge angle than is found for higher Mach numbers. The measured oblique shock angles increase with increasing wedge angle and decrease with increasing Mach number; each of these effects mirrors the behavior of typical fluids. For the purpose of comparison to typical fluids, however, the oblique shock angle in granular materials is much less sensitive to the flow velocity than the oblique shock angle in air; this phenomenon has been noted by Wassgren, *et. al.* [23] and commented on further by Bharadwaj, *et. al.* [24].

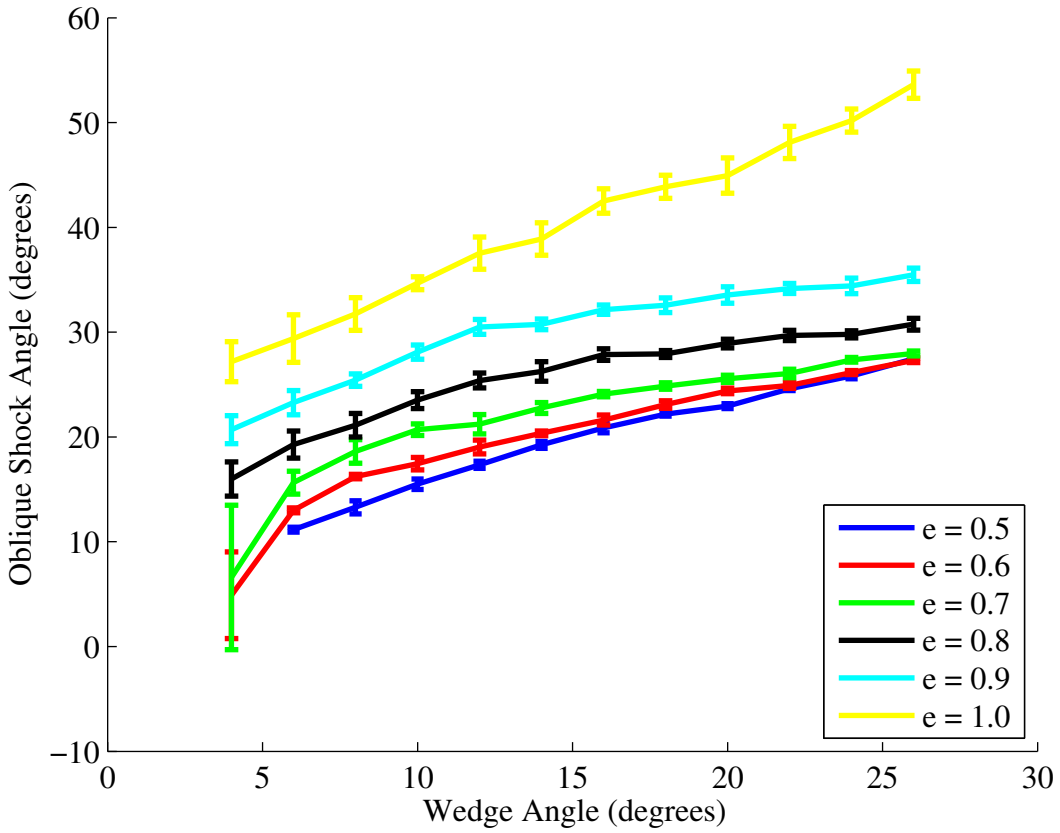

FIG. 5. (Color Online) The variation in oblique shock angle as a function of wedge angle and coefficient of restitution (e). When viewing this figure in grayscale, note that at a wedge angle of 10^o, the curves proceed as follows from top to bottom: $e = 1.0, 0.9, 0.8, 0.7, 0.6, 0.5$, respectively.

Figure 5 shows the measured oblique shock wave angle over a wedge as the coefficient of restitution describing collisions is varied. We note that the oblique shock angle is much more sensitive to the coefficient of restitution than it is to the actual flow velocity. The coefficient of restitution represents a mechanism by which the granular system can experience a decrease in momentum (and therefore energy), and an analog for this in the world of fluid flow is dynamic viscosity; in fact the conservation of momentum is one of the fundamental principles required to formulate the Navier-Stokes equations describing fluid flow and dynamic viscosity is often included in this formulation. The loss of energy characteristic of granular flow is a result of inelastic collisions, and Fig. 5 shows the effect of increasingly inelastic collisions on the bulk behavior of the granular system. For lower coefficients of restitution, the shock wave develops closer to the wedge and for higher coefficients of restitution, the shock wave develops farther from the wedge. Note that the problem of granular collapse, the clustering of

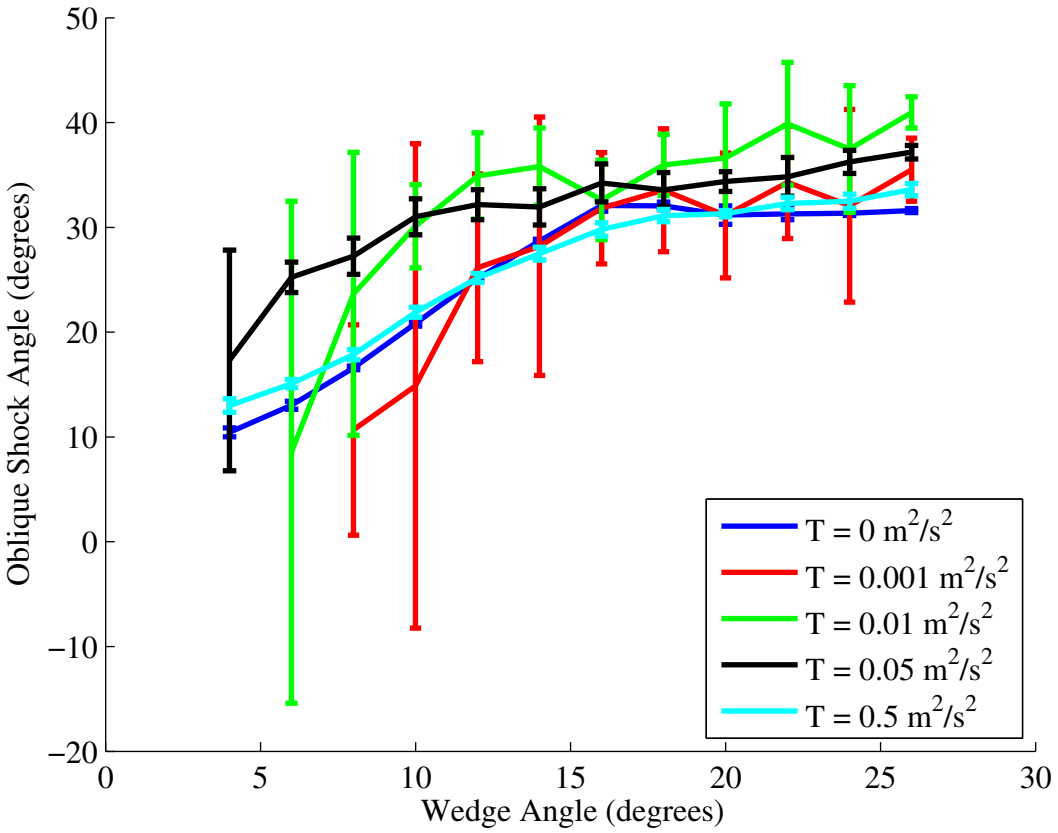

FIG. 6. (Color Online) The variation in oblique shock angle as a function of wedge angle and granular temperature. When viewing this figure in grayscale, note that at a wedge angle of 10^o, the curves proceed as follows from top to bottom: $T = 0.05, 0.01, 0.5, 0, 0.001$ m^2/s^2, respectively.

granular gas constituents often observed in simulations with lower coefficients of restitution [25], is overcome by the periodic nature of the inflow and outflow boundaries. Particle velocities are resampled as they are moved from the outflow to the inflow boundary, and thus the average upstream energy distribution varies little.

Because of the periodic nature of the simulation boundary conditions, particles which lose energy as a result of collisions gain energy when they are reintroduced to the simulation and the simulation avoids the problem of granular collapse or large-scale spatial segregation of particles as has been observed in some granular flow regimes.

Figure 6 shows the variation of the measured oblique shock angle as the initial granular temperature is varied. The granular temperature is a measure of the variance in the particle velocity in each direction. An upstream granular temperature of zero is possible for particle velocities that are all equal; a granular temperature of zero results in an infinite Mach number

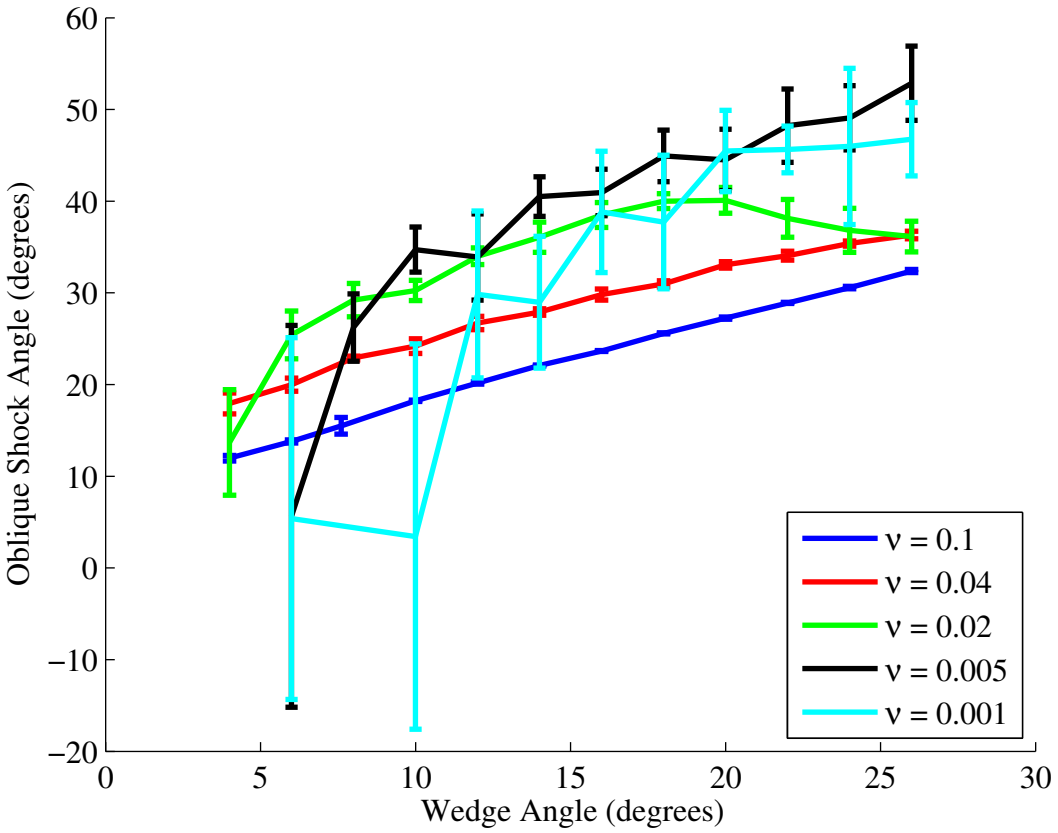

FIG. 7. (Color Online) The variation in oblique shock angle as a function of wedge angle and initial volume fraction. When viewing this figure in grayscale, note that at a wedge angle of 10^o, the curves proceed as follows from top to bottom: $v = 0.005, 0.02, 0.04, 0.1, 0.001$ m/s, respectively.

and thus an interesting condition at which to investigate the upper bound of supersonic flow velocities. Figure 6 shows that the measured oblique shock angle is largely insensitive to the initial granular temperature.

Figure 7 shows the variation of the oblique shock angle as the initial volume fraction of the granular flow is varied. The state of a granular material is highly dependent on volume fraction, and granular systems typically behave as gases at low volume fractions, and as solids at relatively high volume fractions. In the area between gases and solids, the behavior of granular systems is dependent on both the volume fraction and factors such as the rate of energy loss in granular collisions typically characterized by parameters which describe the collision frequency and the average rate of energy addition to the system, among others [26]. Figure 7 shows that the measured oblique shock wave angle is somewhat sensitive to the

initial volume fraction. Comparing Fig. 7 to Fig. 6 and Fig. 5, we observe that the initial volume fraction has a stronger effect on the measured oblique angle than initial granular temperature, but a weaker effect than coefficient of restitution. We also observe that the error associated with the oblique shock measurements for lower volume fractions is greater than the corresponding error associated with higher volume fractions.

B. Flow Past a Disk

The flow of a granular system over a two-dimensional disk provides information about the structure of detached granular shock waves. The formation of shock waves due to supersonic blunt bodies has been of interest to the aerodynamics community since the early days of supersonic flight; the historical significance of bow shocks in the development of ballistic missiles is detailed by Anderson [27] and is a common story in the lore of supersonic aerodynamics. We show the development of the granular analog to supersonic flow impinging on a two-dimensional disk. An example of the resulting bow shock is shown in Fig. 8. Again we note that variation of color (non-uniformity in shading upstream) prior to impact and maintain that it is small compared to the energy decrease at the shock. We parameterize the bow shock using two figures of merit: the distance between the disk and the shock wave in the direction of the average flow (known as the standoff distance) and the angle that the shock forms with the average flow direction outside of the neighborhood of the disk.

Figure 9 shows that the standoff distance decreases with increasing upstream average flow velocity, but is relatively insensitive to the size of the disk obstructing flow. We note that this is to be expected since as long as the disk radii are sufficiently small, the results should approximate a continuum theory, and hence show a relatively flat variation with respect to the radius of the disk.

Figure 10 shows that the standoff distance tends to increase with increasing coefficient of restitution. As with the oblique shock angle in the case of the wedge, a coefficient of restitution of 1.0 results in behavior that deviates from the behavior of systems with lower coefficients of restitution (see Fig. 5). Completely elastic collisions result in standoff distances that generally increase rather than remaining constant with increasing particle size. The error associated with the standoff distance calculation tends to increase with increasing coefficient of restitution. Particles impacting both the impinging disk and other particles

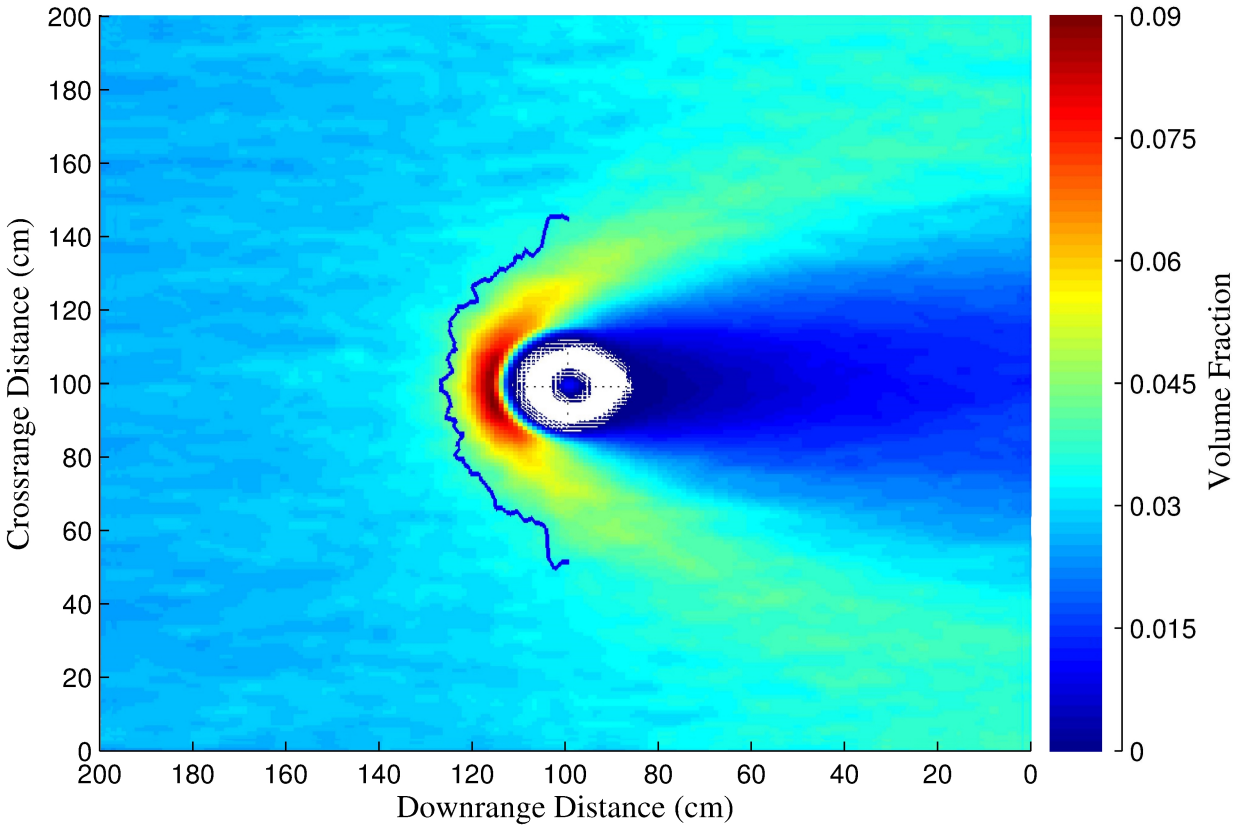

FIG. 8. (Color Online) An example of a bow shock resulting from supersonic granular flow past a disk. The estimated shock position shown by the shock detection algorithm is shown. As in Figs. 1 and 3, color (shading) indicates the local average volume fraction as calculated at each grid point The largest volume fraction is concentrated just upstream of the disk and the lowest volume fraction follows immediately downstream.

in the flow leave the collision with much more energy than those with lower coefficients of restitution; thus the shock wave generated by the disk has a larger spatial range with larger coefficients of restitution.

Figure 11 shows the behavior of the standoff distance as upstream granular temperature is varied. Since upstream granular temperature has a large effect on the Mach number of the system, the resulting Mach number of the flow is also shown. As in the case of flow over a wedge, monodisperse particle velocities result in a granular temperature of zero and, therefore, a flow of infinite Mach number; infinite Mach number flows provide a theoretical boundary to shock behavior. Figure 11 shows that as the granular temperature increases, the Mach number also increases and the measured standoff distance decreases. As with

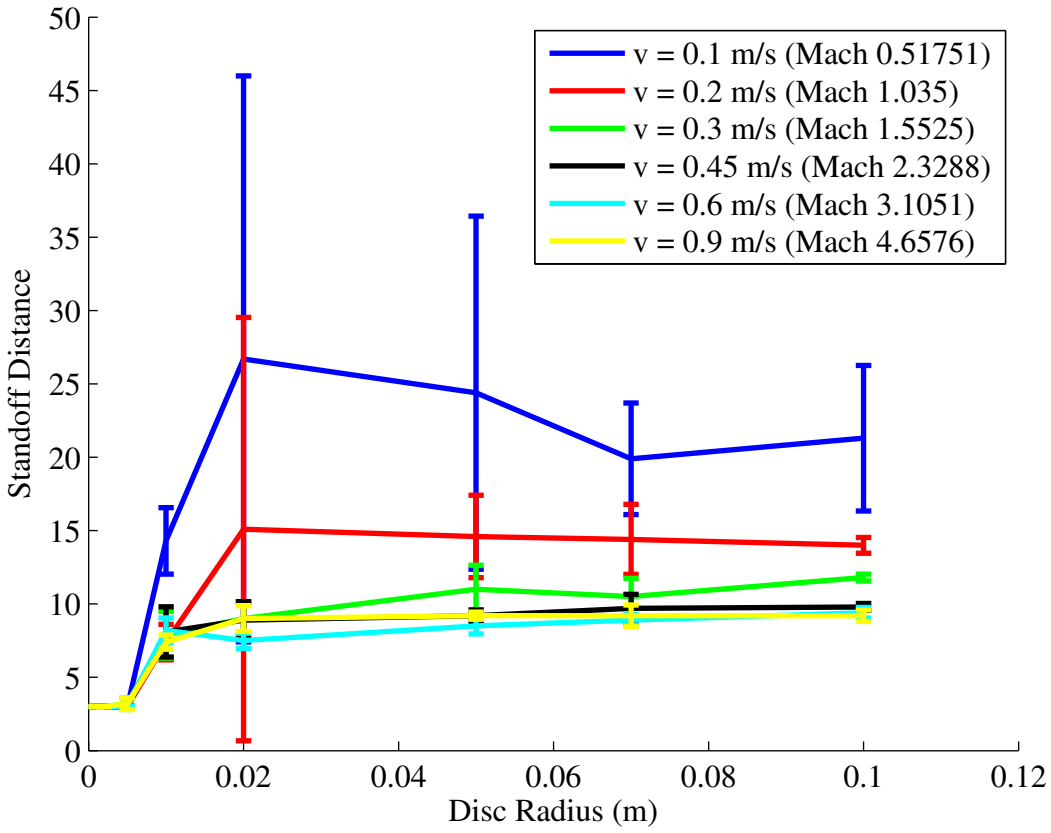

FIG. 9. (Color Online) The variation in standoff distance as a function of disk radius and upstream average velocity. When viewing this figure in grayscale, note that at a disk radius of 0.06 m, the curves proceed as follows from top to bottom: $v = 0.1, 0.2, 0.3, 0.45, 0.9, 0.6$ m/s, respectively.

variations in both coefficient of restitution and velocity, the standoff distance is not sensitive to disk size.

Figure 12 shows that the standoff distance increases with increasing volume fraction, which agrees with experiment [28]. For low volume fraction, which behave like rarefied gases, the standoff distance increases slightly with increasing disk size. For high volume fractions, the standoff distance slightly decreases with increasing disk size, but the error associated with determining the shock wave location increases drastically. We posit that this increase in shock wave error is due to the less gas-like behavior of the granular system as volume fraction increases.

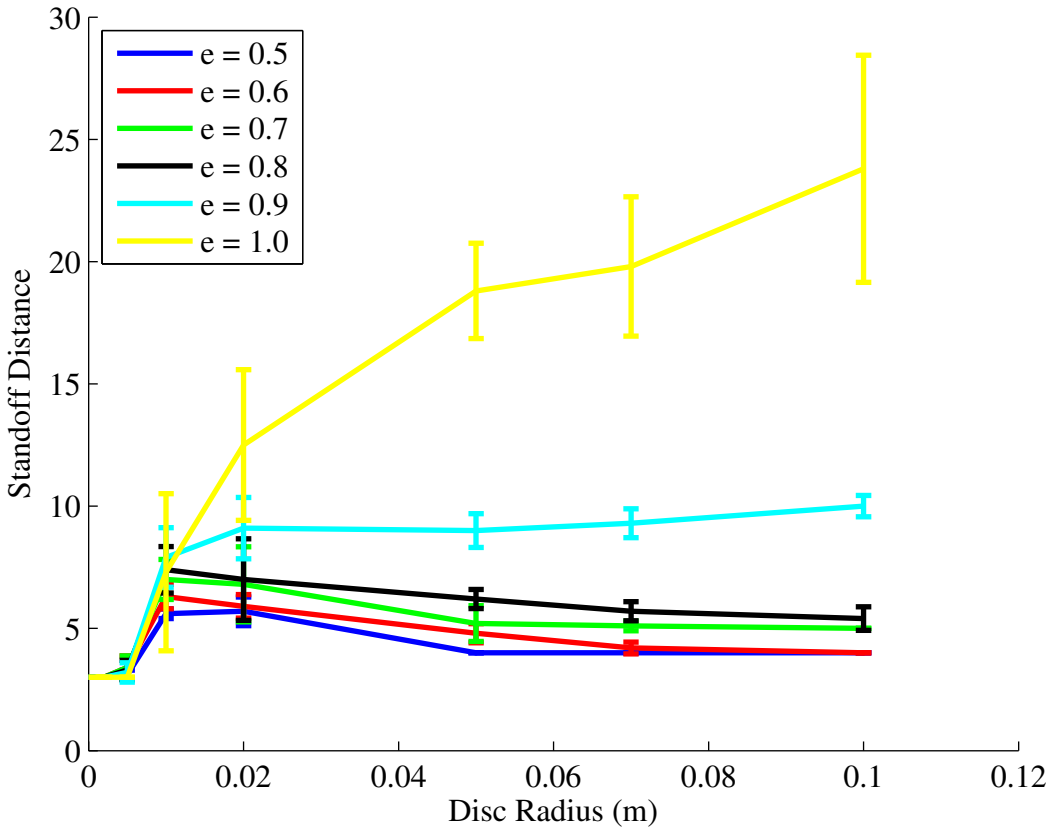

FIG. 10. (Color Online) The variation in standoff distance as a function of disk radius and coefficient of restitution. When viewing this figure in grayscale, note that at a disk radius of 0.06 m, the curves proceed as follows from top to bottom: $v = 1.0, 0.9, 0.8, 0.7, 0.6, 0.5$ m/s, respectively.

V. CONCLUSIONS

The study of granular systems has been of interest both because of the theoretical challenges of describing such systems and because of their myriad practical applications. This paper seeks to use a simple model of granular systems in order to investigate the behavior of supersonic granular flow over two types of impediments: wedges, which lead to the development of oblique shock waves, and disks, which lead to the development of detached bow shock waves. We vary the upstream volume fraction, the upstream granular temperature, the average upstream velocity, and the coefficient of restitution describing the collisions characterizing the granular system to examine the effect of these variations on the oblique shock wave angle (for flow past a wedge) and the standoff distance of detached bow shock waves (for flow past a disk). The results of the research presented indicate that for flow past

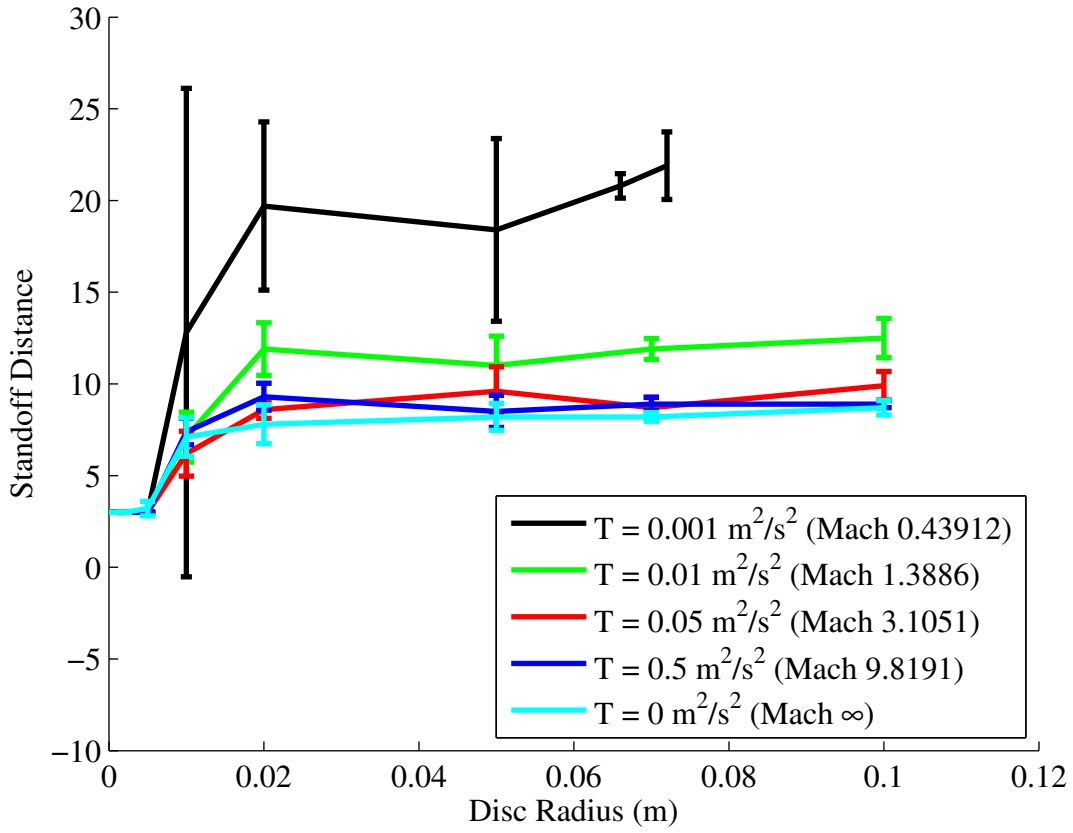

FIG. 11. (Color Online) The variation in standoff distance as a function of disk radius and upstream granular temperature. When viewing this figure in grayscale, note that at a disk radius of 0.06 m, the curves proceed as follows from top to bottom: $v = 0.001, 0.01, 0.05, 0.5, 0$ m/s, respectively.

a wedge, the oblique shock wave angle is strongly affected by the coefficient of restitution characterizing collisions in the granular system; however, unlike for typical gas systems, the average upstream flow velocity (and thus Mach number) and the granular temperature do not strongly affect the oblique shock wave angle. These observations are consistent with experimental observations; however, it is important to note that shocks may be non-unique for the same upstream conditions and wedge angles [5, 7]. This will need to be considered for future studies. The oblique shock wave angle is also influenced by the upstream volume fraction, although the influence of volume fraction is less than that of coefficient of restitution. Similar results are found in the standoff distance for bow shock waves; the upstream volume fraction of the system and the coefficient of restitution have strong effects on the standoff distance, while granular temperature and upstream average flow velocity do not have large effects.

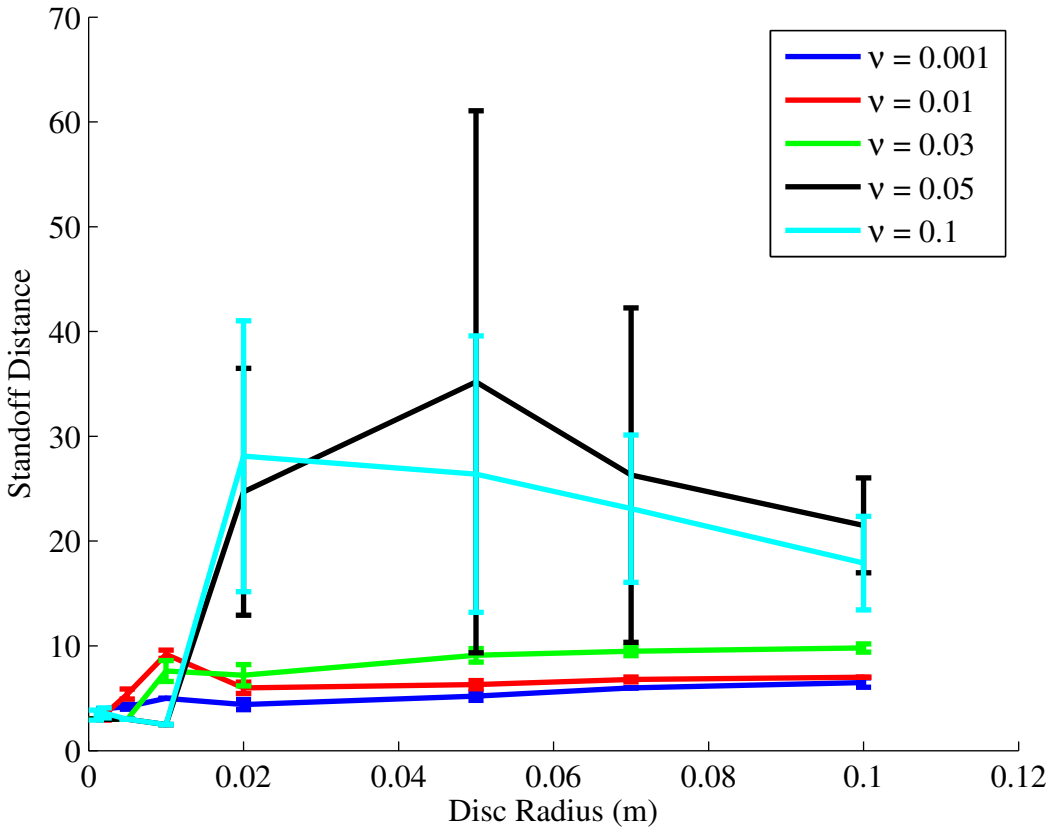

FIG. 12. (Color Online) The variation in standoff distance as a function of disk radius and coefficient of restitution. When viewing this figure in grayscale, note that at a disk radius of 0.06 m, the curves proceed as follows from top to bottom: $v = 0.01, 0.001, 0.03, 0.05, 0.1$ m/s, respectively.

The work presented in this paper represents preliminary results in our study of the physics of granular gases, particularly the physics of shock waves in granular systems. We expect that the data presented in this paper can be used to test theories of granular gases, perhaps to help reconcile observed differences between experimental observations and granular theories [29]. The results presented in this paper can also be used to investigate models of air flow which use event-driven simulations similar to the one used to describe simplified granular flow.

VI. ACKNOWLEDGEMENTS

ACKNOWLEDGMENTS

We gratefully acknowledge support from the National Aeronautics and Space Administration and the North Carolina Space Grant Consortium. We would also like to thank Rodney Metoyer for his assistance with preparing the figures used in this paper.

---

[1] E. Rericha, C. Bizon, M. Shattuck, and H. Swinney, Physical Review Letters **88**, 14302 (2001).

[2] A. Goldshtein, M. Shapiro, and C. Gutfinger, Journal of Fluid Mechanics **316**, 29 (1996).

[3] J. Bougie, S. Moon, J. Swift, and H. Swinney, Physical Review E **66**, 51301 (2002).

[4] A. Benjamin and B. Source, Physics of Fluids **20**, 056601 (2008).

[5] X. Cui and J. M. N. T. Gray, Geophysical Research-Earth Surface **112**, F04012 (2007).

[6] C. G. Johnson and J. M. N. T. Gray, Journal of Fluid Mechanics **675**, 87 (2011).

[7] J. M. N. T. Gray and X. Cui, Journal of Fluid Mechanics **579**, 113 (2007).

[8] A. W. Vreman, M. Al-Tarazi, and J. A. M. Kuipers, Journal of Fluid Mechanics **578**, 233 (2007).

[9] H. Jaeger, S. Nagel, and R. Behringer, Reviews of Modern Physics **68**, 1259 (1996).

[10] J. D. Anderson, *Fundamentals of Aerodynamics*, 4th ed. (McGraw-Hill, New York, 2001) ISBN 978-0072373356.

[11] J. Gray, Y. Tai, and S. Noelle, Journal of Fluid Mechanics **491**, 161 (2003).

[12] P. Heil, E. Rericha, D. Goldman, and H. Swinney, Physical Review E **70**, 060301 (2004).

[13] K. Hákonardóttir and A. Hogg, Physics of Fluids **17**, 077101 (2005).

[14] Y. Amarouchene and H. Kellay, Physics of Fluids **18**, 031707 (2006).

[15] M. Chiou, Y. Wang, and K. Hutter, Acta mechanica **175**, 105 (2005).

[16] A. Levy and M. Sayed, Physics of Fluids **19**, 023302 (2007).

[17] A. Soleymani, P. Zamankhan, and W. Polashenski Jr, Applied Physics Letters **84**, 4409 (2004).

[18] V. Buchholtz and T. Pöschel, Granular Matter **1**, 33 (1998).

[19] H. Herrmann and S. Luding, Continuum Mechanics and Thermodynamics **10**, 189 (1998).

[20] E. Rericha, *Shocks in Rapid Granular Flows*, Ph.D. thesis, University of Texas at Austin (2004).

[21] S. B. Savage, Journal of Fluid Mechanics **194**, 457 (1988).

[22] S. Torquato, B. Lu, and J. Rubinstein, Journal of Physics A: Mathematical and General **23**, L103 (1990).

[23] C. Wassgren, J. Cordova, R. Zenit, and A. Karion, Physics of Fluids **15**, 3318 (2003).

[24] R. Bharadwaj, C. Wassgren, and R. Zenit, Physics of Fluids **18**, 043301 (2006).

[25] J. Rajchenbach, Advances in Physics **49**, 229 (2000).

[26] S. Esipov and T. Pöschel, Journal of Statistical Physics **86**, 1385 (1997).

[27] J. Anderson, in *Computational Fluid Dynamics*, edited by J. F. Wendt (Springer Berlin Heidelberg, 2009) pp. 3–14.

[28] J. Boudet, Y. Amarouchene, and H. Kellay, Physical Review Letters **101**, 254503 (2008).

[29] A. Goldshtein, A. Alexeev, and M. Shapiro, Granular Gas Dynamics , 187 (2003).